

Case Study of Optimized Cascaded Phase Change Thermal Energy Storage Unit

Xu Qiao, Xiangfei Kong* and Long Hao

Tianjin Key Laboratory of Clean Energy Utilization and Pollutant Control, School of Energy and Environmental Engineering, Hebei University of Technology, Tianjin 300401, China

Abstract: Phase change materials are paid increasing attention by the scholars in the past decades. For maintaining a relatively constant renewable energy output as a competent alternative for fossil fuel replacement, phase change storage unit are widely studied. However, for better pursuit of thermal energy performance and energy efficiency, only single staged phase change storage unit is not enough for increasing thermal requirements. Therefore, a triple staged phase change thermal energy storage unit have been proposed in this study. Meanwhile, correspondent comparison with single staged counterpart have been conducted along with related optimization. It has been concluded that the proposed thermal storage unit achieved 334.95 J/s & 41.54% / 186.37 J/s & 53.22 % in thermal energy exchange rate & exergy efficiency during endothermic/exothermic respectively. 3/21.4 L/min are the optimal circulating heat transfer fluid flowrates for endothermic/exothermic (better discharging rate)/ exothermic (better energy efficiency). Moreover, 100/9/15 are the best temperatures of circulating water for endothermic/ exothermic (better discharging rate)/ exothermic (better energy efficiency).

Keywords: Cascaded thermal energy storage unit, Phase change material, System optimization, Energy efficiency, Exergy efficiency.

1. INTRODUCTION

Social continuous development (Ruggerio, 2021) is quite important for modern global development, and it will be continuously be playing an essential role in future flourishing. As long as the environment sustainability of human society is still a necessity, authorities would be asked to be caring for doing so. However, given the sustainable development requirement, the building section accounts for over 30 % (Somu, Raman M R, & Ramamritham, 2021) of the total energy consumption, among which, living condition maintaining is yet consuming almost a half (Sukarno, Putra, Hakim, Rachman, & Indra Mahlia, 2021), signifying the huge potential in energy conservation. Therefore, given the primary social operation is basically depending on fossil fuels, energy-saving is attracting increasing attention.

Herein, apart from the non-renewable energy, alternatives (Levenda, Behrsin, & Disano, 2021) have been being searched for so long. For example, solar energy (Rabaia *et al.*, 2021), wind energy (Ahmed, Al-Ismaail, Shafiullah, Al-Sulaiman, & El-Amin, 2020), hydropower (K. Kumar & Saini, 2022) and tidal energy (Neto, Saavedra, & Oliveira, 2020) etc. As for solar energy, relative techniques have been developed quite well, and serial standard derivative products have been made by the manufacturer. Though, solar energy is free of charge, clean and renewable, its intermittency (Manohar, Koley, Ghosh, Mohanta, & Bansal, 2020)

and fluctuating intensity (Nukulwar & Tungikar, 2021) are troubling the researchers in its relevant all-weather applications around the clock.

Taken this into consideration, phase change thermal energy storage technology (Jouhara, Żabnieńska-Góra, Khordehghah, Ahmad, & Lipinski, 2020) has come into the sight of the scholars. Possessing sufficient excellent properties such as, abundant energy storage capacity/density, relative temperature consistency within the phase change duration, acceptable physiochemical stability, significant plasticity, non-corrosive and non-toxicity etc., phase change material (PCM) (Zhang *et al.*, 2021) has been one of the favorites among the research topics towards the future sustainable development. Based on the outstanding nature of solar energy and PCM, the idea of combining them two came up to the researchers' minds. Consequently, all kinds of PCMs have been studied throughout these years, organic ones, inorganic ones and mixed types.

And as concluded by the colleagues working on relevant fields, phase segregation (Soni, 2021) and sub-cooling (Cao, Luo, Han, Lu, & Zou, 2022) are main impact factors restraining the inorganic PCM from large-scale utilization. On the contrary, organic PCM (Singh *et al.*, 2021) being able to provide acceptable phase change temperature, enough latent heat, proper thermal capacity and other adoptable thermal parameters, it has been preferred than the former, especially in building related applications. Subsequently, for the sake of building indoor environment conditioning, solar energy system has been coupled with PCM aiming at alleviating solar intermittency and its varying intensity, also electric

Address correspondence to this article at the Tianjin Key Laboratory of Clean Energy Utilization and Pollutant Control, School of Energy and Environmental Engineering, Hebei University of Technology, Tianjin 300401, China; Tel./Fax: +86 2260435279; E-mail: xfkong@hebut.edu.cn

heating (Ma, Bao, & Roskilly, 2020) would be adopted for extra energy demand. Lots of researches have been conducted over solar heating/cooling with PCM (Qiao, Kong, & Fan, 2022), both with organic (Pasupathi, Alagar, P, M.M, & Aritra, 2020) and inorganic (R. R. Kumar *et al.*, 2022) PCMs. For instance, G. Raam Dheep *et al.* (Dheep & Sreekumar, 2018) tested an organic PCM (glutaric acid) for solar heating application, of which the PCM changes phase around 94.97–99.2 °C with a enthalpy of 184.8 J/g, and proved their proposal to be effective for such purpose. Md. Also, Hasan Zahi *et al.* (Lancet & Pecht, 1977) tested a polyethylene glycol to be competent for thermal energy storage with a thermal conductivity of 0.51 W/m·K and latent heat of 146 J/g. However, the organic PCMs suffer from low thermal conductance, for which thermal additives are needed for relevant thermal enhancement, limiting correspondent deployments of the organic PCMs. For the inorganic PCM, compared with the former, relative acceptable thermal conductivity are preferred. Moreover, when subcooling and phase segregation are solved, it would be quite competing in thermal energy storage. P. Manoj Kumar *et al.* (Manoj Kumar *et al.*, 2023) attempted to deal with the subcooling problem of sodium acetate trihydrate ($\text{CH}_3\text{COONa}\cdot 3\text{H}_2\text{O}$) with 0.75 % nano-MgO particles, and it turns out that the PCM was 40.39 % in thermal conductivity along with 0.32 °C in modified supercooling. Additionally, Xiaohua Bao *et al.* (Bao *et al.*, 2020) tried to improve the phase segregation of $\text{CaCl}_2\cdot 6\text{H}_2\text{O}$ by adding 0.5 wt% flake graphite, which results in not only improvement in phase separation, but also enhancement in thermal conducting performance (13.8 % enhanced) and overcooling (less than 1 °C). Generally speaking, PCMs are adopted based on their thermal performance, both organic/inorganic ones. Xu Qiao *et al.* (Qiao, Kong, Li, Wang, & Long, 2020) experimentally and numerically studied a solar active wall heating system with paraffin (25 °C), and results indicates that the proposed system is practical for building heating purpose, along with relative optimization conducted. And Salem Algarni *et al.* (Algarni *et al.*, 2020) integrated the PCM with solar collector using paraffin, and the system efficiency was 32 % improved by adding nano copper particles to the PCM. Apart from the PCM application to solar collector (heat source) and building parts (demand side), thermal energy storage unit as an essential component of the heating distribution network, also has been widely researched for combination with PCM. Bilal Lamrani *et al.* (Lamrani, Kuznik, & Draoui, 2020) investigated a paraffin (RT-55) filled thermal storage unit combined solar heating system for large buildings. Results showed that the proposed system was able to provide 85-36 / 63-38 °C, during daytime / nighttime, respectively. Mingyang Huang *et al.* (Huang *et al.*, 2022) did an experiment on paraffin thermal storage

unit installed solar heating system, and they finally achieved a relative high temperature difference between the internal and external surface of the unit, along with the PCM receive heating power was stable at 6-8 kW under the heating condition of 85 °C.

Besides the afore-mentioned studies, only single PCM integration with the solar heating system is not enough sometimes, especially for extreme weather and higher energy efficiency. As a result of this, thermal energy storage in cascaded mode has been raised. Therefore, to tackle this, Hamidreza Shamsi *et al.* (Shamsi, Boroushaki, & Geraei, 2017) proposed a triple PCM cascading thermal storage unit, and they concluded there was a 5 % promotion in thermal energy storage/release when comparing with systems with single PCM. Moreover, Saeed Nekoonam *et al.* (Nekoonam & Ghasempour, 2021) explored a cascaded thermal energy storage solar heating system by employing RT50, RT65 and RT80. And it proved 12 % improvement in thermal performance for multi-PCM thermal storage versus single-PCM counterpart.

In this study, a novel three stage thermal storage unit is put forward, which is composed of erythritol/urea (Er-U), $\text{CH}_3\text{COONa}\cdot 3\text{H}_2\text{O}$ (SAT) and $\text{Na}_2\text{SO}_4\cdot 10\text{H}_2\text{O}$ (SSD), of which the phase change temperatures are 78/58/32 °C. For the organic PCM, its low thermal conductance has been modified via additives and the supercooling/phase segregation have also been dealt with. After that, the triple-staged thermal energy storage unit (TS-TESU) have been optimized in configuration for better thermal performance.

2. EXPERIMENTAL SET-UP

2.1. Material Preparation

First stage: In order to get the proper phase change temperature, erythritol (Ery) and urea (Ur) are mixed through melt-blending polymerization, in 60/40 wt% ratio. And expanded graphite is introduced to it via vac-sorb method for its supercooling and thermal conductivity improvement.

Second stage: SAT was chosen for the second thermal storage stage, of which, the Sodium pyrophosphate ($\text{Na}_4\text{P}_2\text{O}_7\cdot 10\text{H}_2\text{O}$, SP) as nucleating agent and expanded graphite (EP), was adopted for supercooling by mixing them directly.

Third stage: SSD was employed for the third stage, Sodium borate ($\text{Na}_2\text{B}_4\text{O}_7\cdot 10\text{H}_2\text{O}$, Sb) was introduced for its overcooling as nucleating agent.

Corresponding parameters of the prepared composites are listed below in Table 1. And all the

Table 1: Thermal Parameters of PCMs Prepared

No.	Material	Onset phase change temperature		Latent heat (J/g)		Thermal conductivity (W/(m·K))	Specific heat (J/(g·°C))	Density (kg/m ³)
		Onset melting point (°C)	Onset solidifying point (°C)	Melting	Solidifying			
1	Ery/Urea/EP	80.64	73.03	255.9	236.65	1.912	1.785	1422
2	CH ₃ COONa·3H ₂ O	59.45	58.61	282.73	251.54	0.814	1.973	1384
3	NaSO ₄ ·10H ₂ O/EP	33.18	27.82	128.25	126.26	1.612	1.752	1663

materials mentioned are purchased in analytical grade, which are competent for such experiment.

2.2. Test Rig Configuration

After the material preparation, the test rig was built, which consists of three thermal storage units. Phase change points are 80.64/59.45/33.18 °C in first (high) to third (low) manner. The first, with relatively high phase change temperature,

Three polymethyl methacrylate (PMMA) boxes (200 mm× 200 mm× 200 mm in dimension) are customized for containing the PCMs, inserted by copper coils for heat exchange between heat transfer fluid (HTF, water) and PCMs. In addition, thermal insulation materials are attached to the external surface of them. A thermostat water-bath is deployed as the heat source. Figure 1 shows the test rig system, and Table 2 lists the thermal

properties of the experimental components.

The specific experimental strategies include:

1. Endothermic process: At the beginning, cooling the water inside the thermostat down to 10 °C for 10 min, and then start the pump circulation, cooling all the water flowing through the whole system down to 10 °C for 30 min. This is for ensuring the initial temperature of the system is set to 10 °C. After that, heat up the water in the thermostat to 90 °C for 10 min, and then start water circulation to heat the whole system up to 90 °C.
2. Exothermic process: When endothermic process is accomplished, with which the exothermic process begins. Firstly, cool down the thermostat down to 10 °C for 10 min. And the circulation pump was switched on then, for the thermal



Figure 1: Cascaded thermal energy storage unit system.

Table 2: Thermal Properties of Experimental Components

Material	Thermal conductivity (W/(m·K))	Density (g/cm ³)	Thickness (mm)
PMMA	0.213	1.19	5
Thermal insulation	0.045	0.131	20
Heat transfer coils	379	8.51	1

storage to desuperheat, till the global temperature is cooled down to 10 °C.

3. MATHEMATICAL MODEL

In this study, optimization simulation is carried out for better systemic thermal performance. The mathematical model is established thereby, and the formulae are illustrated below.

Energy:

$$Q = m \cdot C_p \cdot \Delta t \tag{1}$$

$$Q = \sum_{t_1}^{t_2} m \cdot C_p (t_4 - t_3) \cdot \Delta T \tag{2}$$

Where : Q is the thermal energy stored/released by the PCM unit (kJ), m denotes the mass flow rate of water (kg/h), C_p specific heat capacity of water (kJ/(kg·°C) ; Δt signifies the temperature difference between the inlet/outlet of each unit (°C), t₁, t₂ indicate the temperature of PCM (°C), t₃ means inlet temperature of circulating water (°C), t₄ is inlet temperature of circulating water (°C), ΔT is on behalf of the time interval of data acquisition (min) (Verma, Varun, & Singal, 2008).

$$\eta = \frac{Q_2}{Q_1} \times 100\% \tag{3}$$

$$\xi = \frac{Q}{t} \times 100\% \tag{4}$$

Among which:

η is the exergy efficiency of the PCM, Q₁ denotes the amount of stored heat (kJ), Q₂ means the amount of stored heat (kJ), ξ signifies the heat transfer rate of the PCM (kJ/ s), Q indicates the stored thermal energy of PCM (kJ), t stands for the time of thermal storing (s).

$$\eta_1 = \frac{\Delta Ex_{pcm}}{Ex_{in}} = \frac{Ex_{in} - Ex_{out} - \sum L_i}{Ex_{in}} \times 100\% \tag{5}$$

$$\eta_2 = \frac{Ex_{out} - Ex_{in}}{\Delta Ex_{pcm}} \times 100\% \tag{6}$$

Where:

η₁ means exergy efficiency, ΔEx_{pcm} is exergy variation (kJ), Ex_{in} systemic exergy inlet (kJ), Ex_{out} stands for the outlet counterpart (kJ), ΣL_i indicates the exergy dissipation caused by irreversible procedure (kJ) (Sami, Etesami, & Rahimi, 2011).

$$\Delta Ex_{pcm} = \int_{T_{s-i}}^{T_{l-i}} m_i c_{s-i} (1 - \frac{T_0}{T}) dT + \int_{T_{l-i}}^{T_{p-i}} m_i c_{l-i} (1 - \frac{T_0}{T}) dT + m_i r_i (1 - \frac{T_0}{T_{p-i}}) \tag{7}$$

$$Ex_{in} = \int_{T_0}^{T_{in}} m_w c_p (1 - \frac{T_0}{T}) dT \tag{8}$$

$$Ex_{out} = \sum_{j=1}^n \left(\int_{T_0}^{T_j} \Delta m_w c_p (1 - \frac{T_0}{T}) dT \right) \tag{9}$$

Among which:

m_i is the mass of different PCMs respectively (kg), c_{s-i} means the solidus sensible thermal energy of PCMs kJ/(kg·°C), c_{l-i} represents the liquidus sensible thermal energy of PCMs kJ/(kg·°C), r_i stand for latent heat of the PCMs (kJ/kg), T_{s-i} is solidus temperature of the PCMs (°C), T_{l-i} indicates liquidus temperature of the PCMs (°C), T_{p-i} denotes the phase change points of the PCMs (°C), T₀ is on behalf of indoor temperature (°C), j is outlet temperature of unit j (°C), T_j demonstrates the temperature of unit j (°C), Δm_w represents water mass flow rate in every 10 s (kg) (Li, He, Yin, Miao, & Li, 2008).

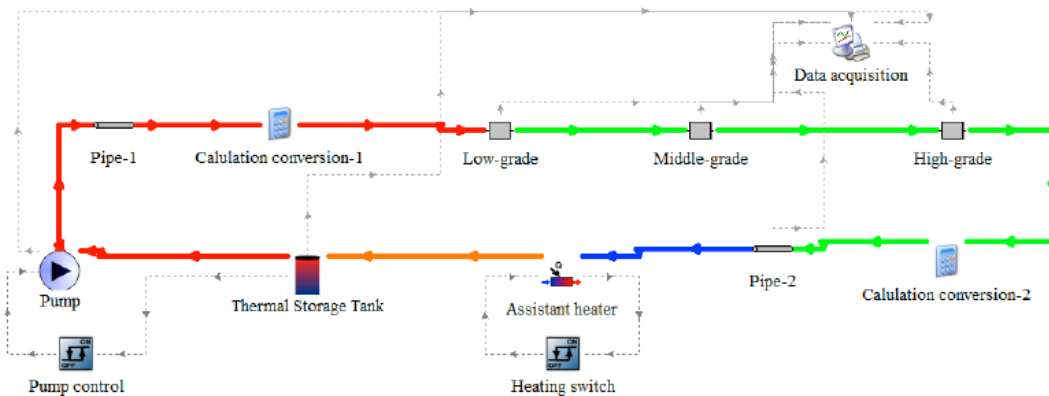


Figure 2: Mathematical model of cascaded thermal energy storage unit.

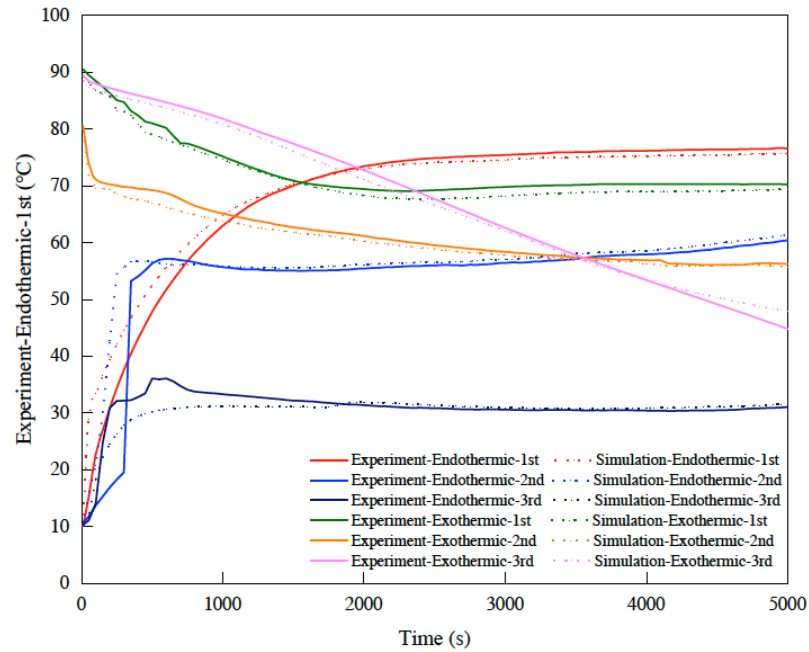


Figure 3: Experimental and simulation data difference.

4. RESULTS AND DISCUSSION

4.1. Model Validation

After the establishment of the simulation model, it is necessary for the model to be validated comparing with the experimental results. Therefore, relative procedures have been conducted. In Figure 2, demonstrates the simulation model of cascaded thermal energy storage unit. And as it can be seen from Figure 3, there is acceptable correlation between experimental and simulated results. Also, according to the standard deviation and variance illustrated in Table 3, the statement can be firmly approved. Based on this, correspondent optimization of the cascaded phase change thermal energy storage unit has been put forward and conducted via transient system simulation program (TRANSYS). Moreover, the first/second/third stage thermal storage unit are expressed as

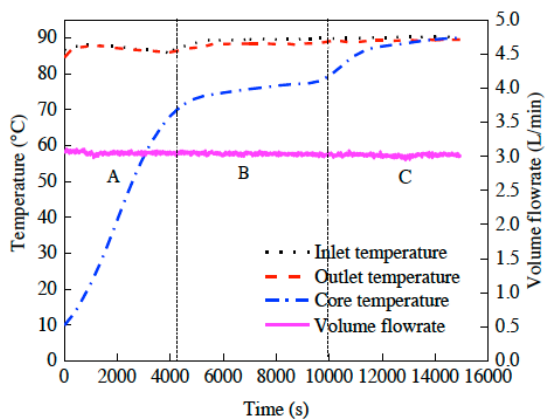
1st/2nd/3rd in short in the figure.

Table 3: Data Difference between Experimental and Simulated Outcome

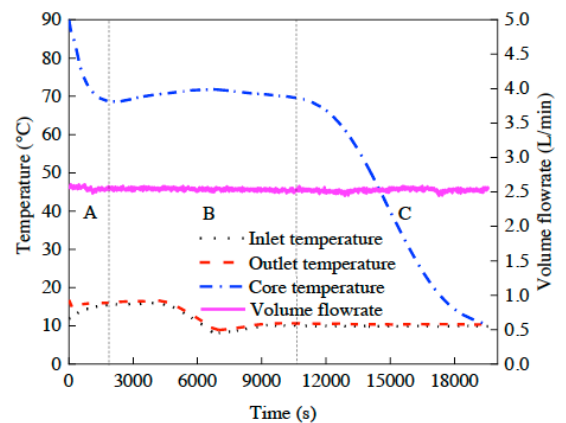
Data Difference	Standard Deviation	Variance
1st Endo	0.01	0.03
2nd Endo	0.01	0.14
3rd Endo	0.01	0.02
1st Exo	0.01	0.01
2nd Exo	0.01	0.01
3rd Exo	0.02	0.05

4.2. Experimental Results

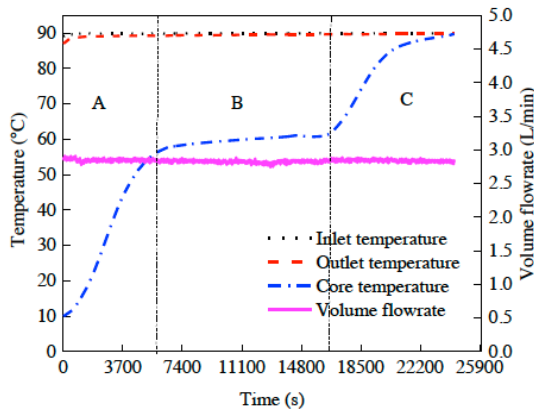
As demonstrated in previous sections of this manuscript, the system configuration and connection have been set forth, along with the operation strategy,



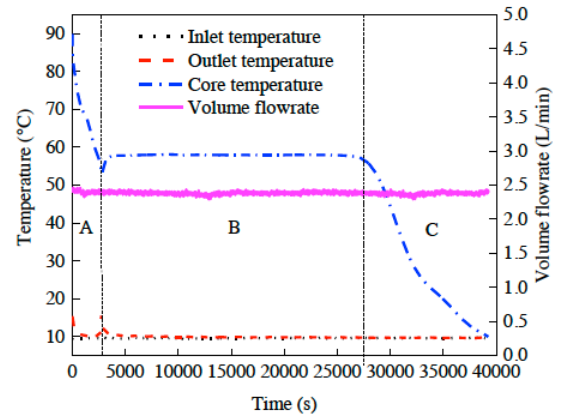
(a) 1st Endothermic process.



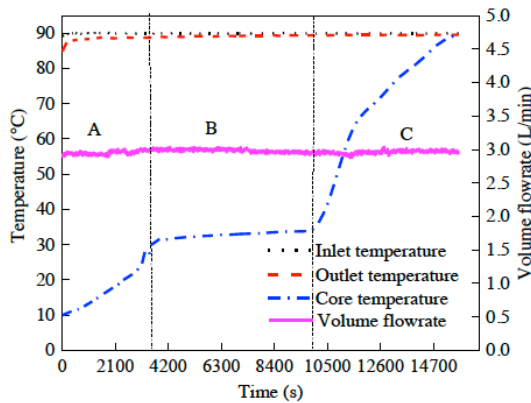
(b) 1st Exothermic process.



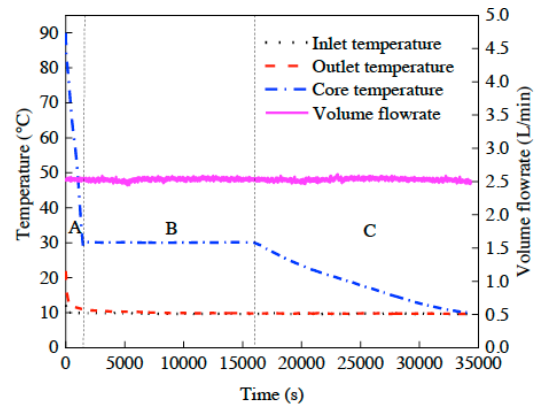
(c) 2nd Endothermic process.



(d) 2nd Exothermic process.



(e) 3rd Endothermic process.



(f) 3rd Exothermic process.

Figure 4: Individual thermal energy storage unit temperature data during endothermic/exothermic process: (a) 1st Endothermic process, (b) 1st Exothermic process, (c) 2nd Endothermic process, (d) 2nd Exothermic process, (e) 3rd Endothermic process, (f) 3rd Exotherm.

the outcomes of the experimental have been obtained. And this part is going to give a brief analysis of them.

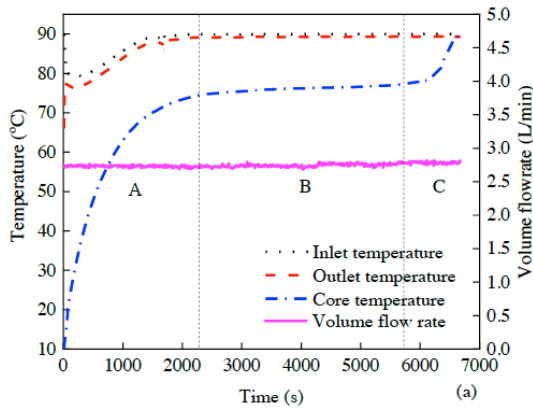
In Figure 4, temperature curves of thermal energy storage in individual mode are shown. And as is shown in Figure 5, temperature variation of the cascaded thermal energy storage unit during endothermic/exothermic process are illustrated. A, C are three sections in the figures indicating sensible heat storage/release processes, and B represents phase change heat transfer process. According to the experiments over thermal energy storage/release of the PCM individual/cascaded unit, the phase change temperatures of the PCMs were almost constant during the two experiments.

Endothermic process: For the first stage, with the endothermic onset temperature at around 75 °C, the phase change period lasted for about 41.31 % of the total duration. Besides, the charging time reduced 8250 s compared with individual unit (Ery/Urea/EP alone). And, for the second stage, whose phase change takes place at about 58 °C, endothermic period accounts for 58.43 % of the whole period. Compared with the single

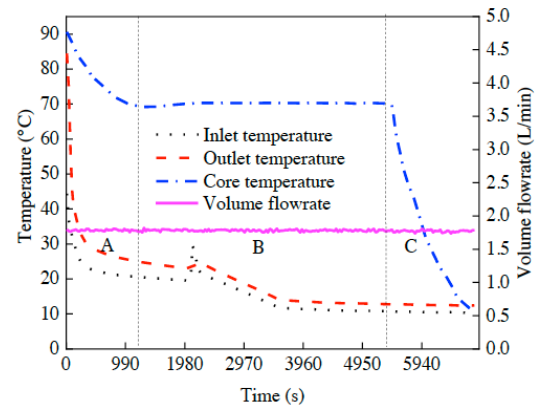
unit ($\text{CH}_3\text{COONa}\cdot 3\text{H}_2\text{O}$ alone), phase change duration was 17630 s decreased for the cascaded phase change unit. After that, when it comes to the third stage, during which 30 °C of temperature triggers its phase change process, and 43.55 % of it was spent on latent heat charging. Additionally, in comparison with individual unit ($\text{NaSO}_4\cdot 10\text{H}_2\text{O}/\text{EP}$ alone), its correspondent phase change was 9010 s shortened for its cascaded counterpart.

Based on the results of endothermic process, it can be concluded that the cascaded arranged phase change temperatures facilitated the heat transfer along the flow direction of heat transfer fluid, significantly speeded up the phase change progress.

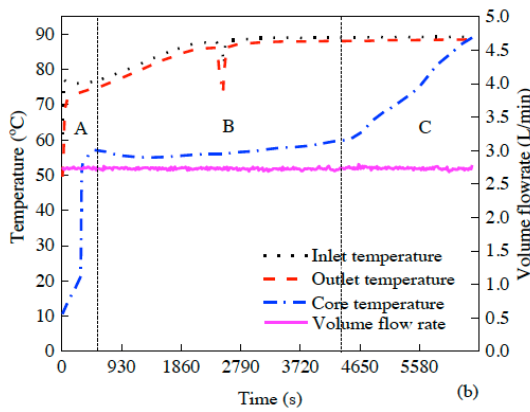
Exothermic process: After discussing the endothermic process, related exothermic procedure are also analyzed. As it can be seen in the figures above, the onset phase change temperatures of each stage are 70/58/26 °C respectively, along with according phase change time duration accounting for 58.94/70.58/46.67 % of the total exothermic process correspondingly. In contrast with the single stage



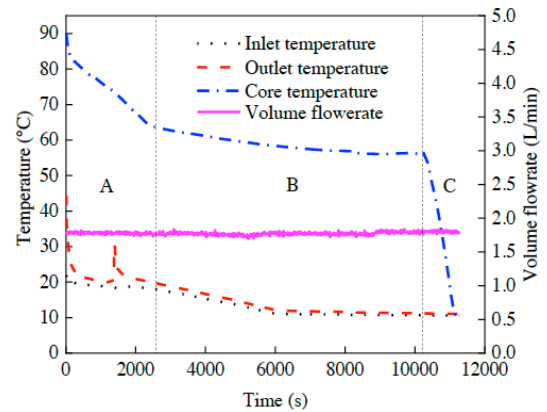
(a) 1st Endothermic process.



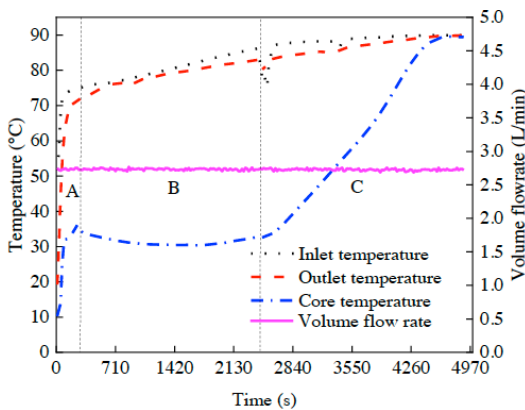
(b) 1st Exothermic process.



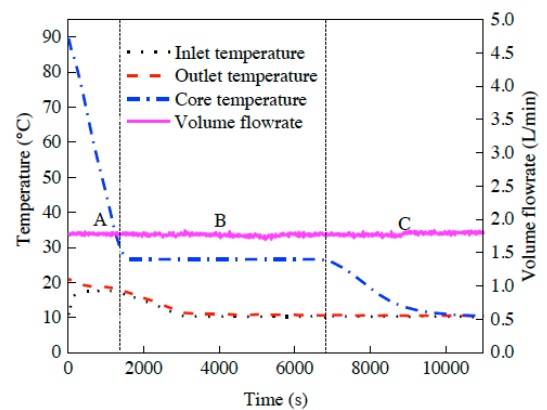
(c) 2nd Endothermic process.



(d) 2nd Exothermic process.



(e) 3rd Endothermic process.



(f) 3rd Exothermic process.

Figure 5: Cascaded thermal energy storage unit temperature data during endothermic/exothermic process: (a) 1st Endothermic process, (b) 1st Exothermic process, (c) 2nd Endothermic process, (d) 2nd Exothermic process, (e) 3rd Endothermic process, (f) 3rd Exotherm.

counterparts, relative phase change periods are shortened by 7540/28220/22330 s for the cascaded phase change unit.

Based on the exothermic process of the comparison between the cascaded/individual thermal storage unit, it can be summarized that the cascaded thermal storage unit achieved relatively constant temperature gradient. Simultaneously, thermal energy flux transfer caused by the temperature gradient was maintained in

intensity. Therefore, compared with the single staged thermal storage unit, the cascaded counterpart possesses strengthened heat exchange performance, *i.e.*, higher thermal efficiency in energy utilization.

4.3. System Optimization Simulation

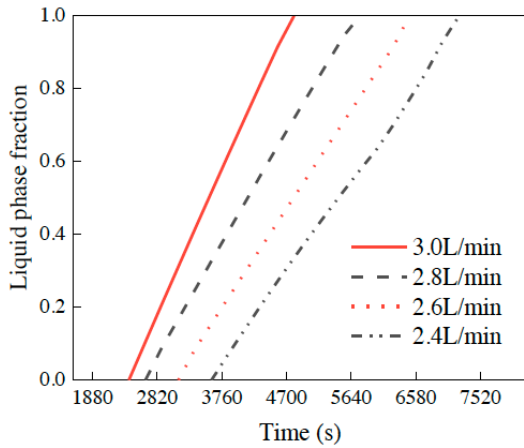
When accomplishing the thermal performance validation in comparison with the single staged thermal energy storage unit, in order to ulteriorly improve the

system performance and explore the systematic optimal configuration/strategy, corresponding mathematical model have been built and optimized via TRANSYS software. And the optimization was carried in two dominant influence factors: volume flowrate and heating temperature of the heat transfer fluid.

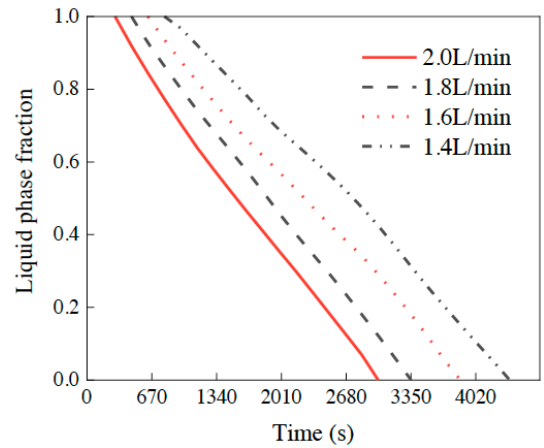
Simulation for optimal HTF flowrate: For the optimization simulation, the operation was the same as

the experiment, temperature was set from 10 °C to 90 °C, and then back down to 10 °C. Four flowrates were chosen for endothermic/exothermic respectively, *i.e.*, 2.4/2.6/2.8/3.0 L/min for the former and 1.4/1.6/1.8/2.0 L/min for the latter. And liquid phase fraction (LPF) was introduced for representing the use ratio of the PCMs.

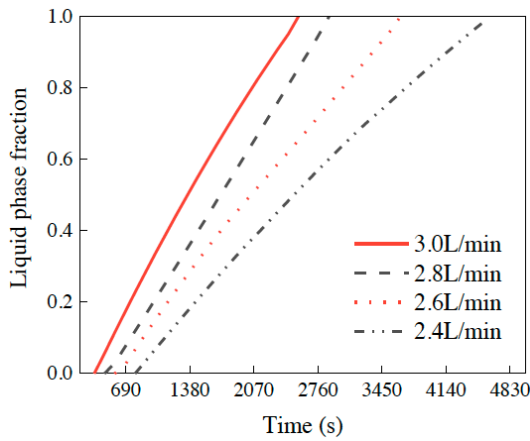
Figure 6 lists the LPF and outlet temperature during endothermic/exothermic processes of the proposed



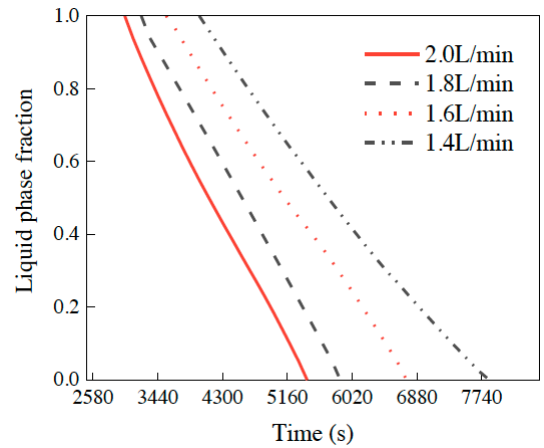
(a) 1st Endothermic



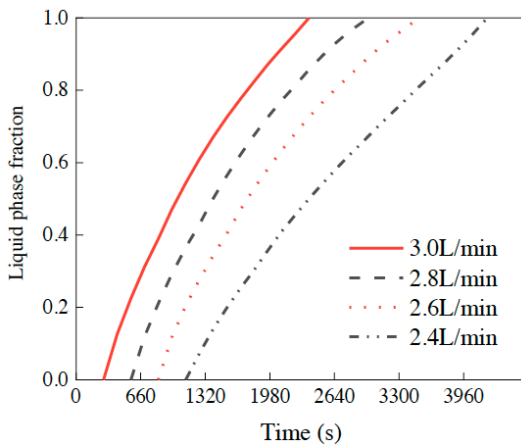
(b) 1st Exothermic



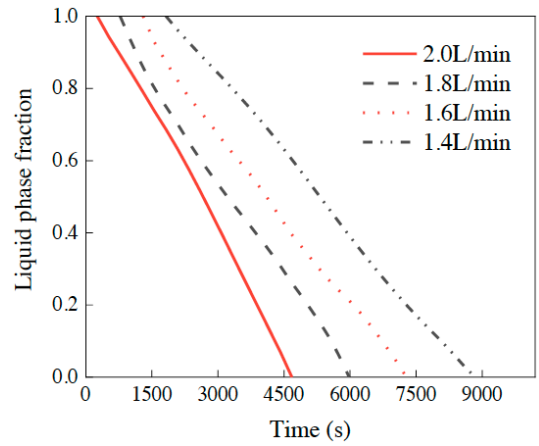
(c) 2nd Endothermic



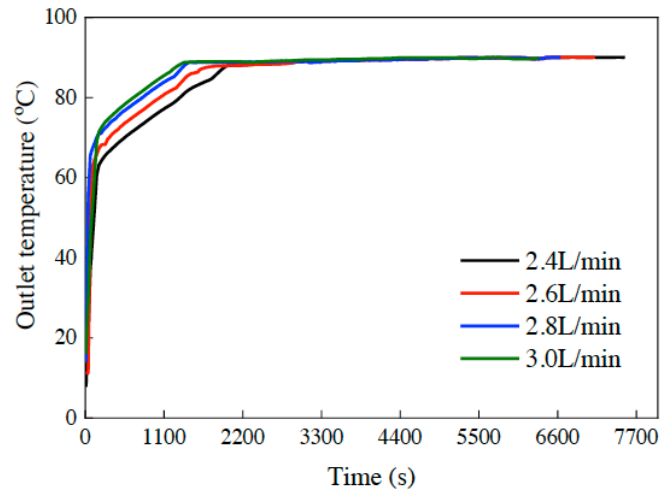
(d) 2nd Exothermic



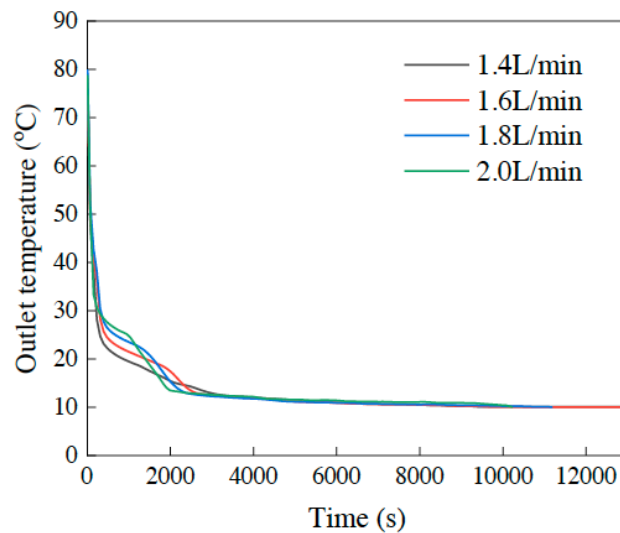
(e) 3rd Endothermic



(f) 3rd Exothermic



(g) Outlet temperature of cascaded thermal energy storage unit during endothermic process.



(h) Outlet temperature of cascaded thermal energy storage unit during exothermic process.

Figure 6: Data of cascaded thermal energy storage unit versus different heat transfer fluid volume flowrates: (a) 1st Endothermic, (b) 1st Exothermic, (c) 2nd Endothermic, (d) 2nd Exothermic, (e) 3rd Endothermic, (f) 3rd Exothermic, (g) Outlet temperature of cascaded thermal energy storage unit during endothermic process, (h) Outlet temperature of cascaded thermal energy storage unit during exothermic process.

cascaded thermal energy storage unit. According to which, the corresponding LPF increases with the temperature rise in circulating water, thereby, making it possible for the storage unit to store more energy. And this facilitates the thermal efficiency in heat transfer, promoting the PCM use ratio, reducing the time consumption during thermal energy exchange. Apart from that, energy charging achieves the utmost value (369.73 J/s) at the flowrate of 3 L/min, which surpasses that of 2.4 L/min by 19.59 %. In addition, exergy efficiency climbs up with the upward variation of heating water flowrate, reaching up to 369.73 J/s at 3 L/min, giving a 42.87 % exceeding than that of 2.4 L/min. Therefore, 3 L/min was chosen as the optimal circulating flowrate of the HTF during endothermic process.

For the exothermic procedure, lower LPF signifies better heat release, and the former presents a negative correlation with the latter. According to Figure 6 (h), 2 L/min was selected as the optimal flowrate for exothermic process when thermal discharging rate is more concerned of. Due to the correspondent heat discharging rate reached 210.93 J/s, 28.34 % faster than that of 1.4 L/min. Moreover, 1.4 L/min would be the best for the cascaded thermal storage unit when system exergy efficiency is more concerned of, for it accomplished a 54.51 % of exergy efficiency at 1.4 L/min.

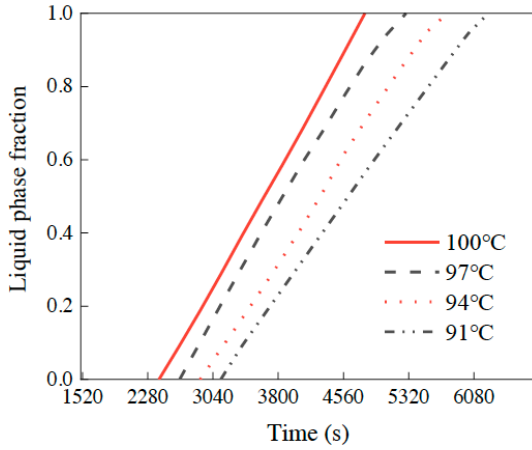
Simulation for optimum HTF temperature: Temperature of the HTF is important for the system thermal performance, making it necessary for relative optimization. Four temperatures are selected for HTF

during endothermic/exothermic processes, *i.e.*, 91/94/97/100 °C for the former and 9/11/13/15 °C for the latter.

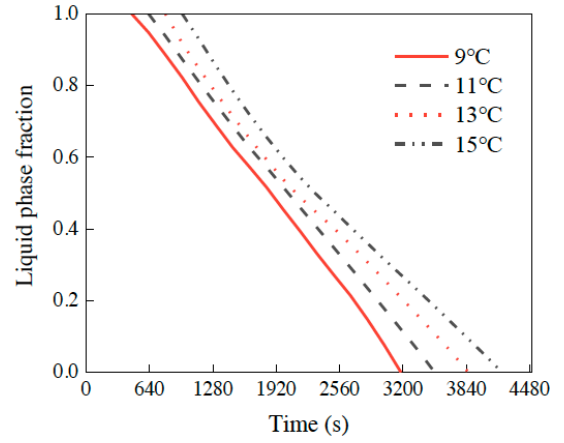
As shown in Figure 7, LPF curves and outlet temperature of the cascaded storage unit are depicted. And hereby, within endothermic process, the higher the heat storage temperature of PCMs with different gradients at the same time, the higher the LPF, which

is because with the increase of heat storage unit temperature, the heat transferred by the HTF to the PCM is faster, which improves the heat storage rate of PCMs and can effectively reduce the heat storage duration, which is also reflected in the increase of LPF.

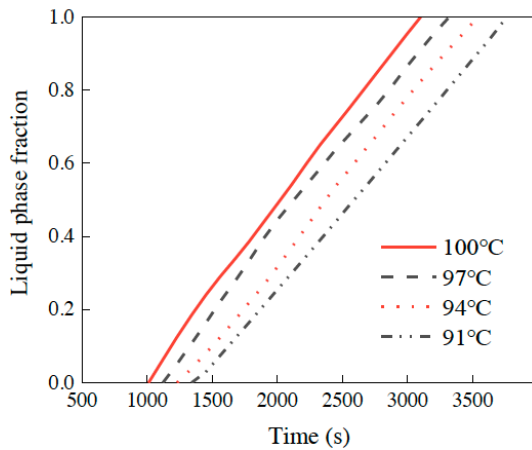
When the inlet water temperature is 100 °C, the charging time is the shortest, with the maximum charging rate of 391.01 J/s. Compared with that of 91



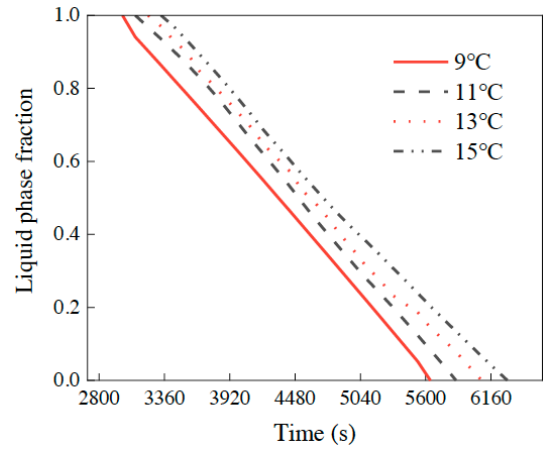
(a) 1st Endothermic



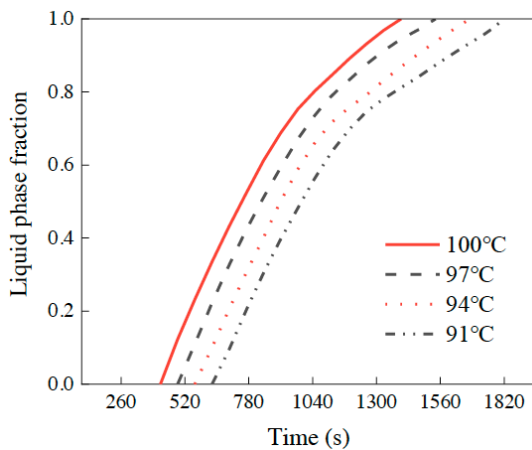
(b) 1st Exothermic



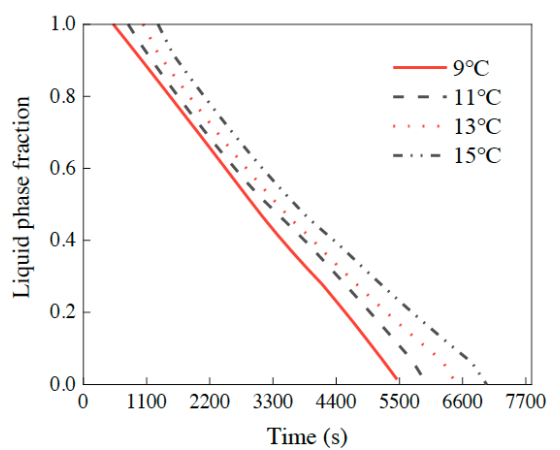
(c) 2nd Endothermic



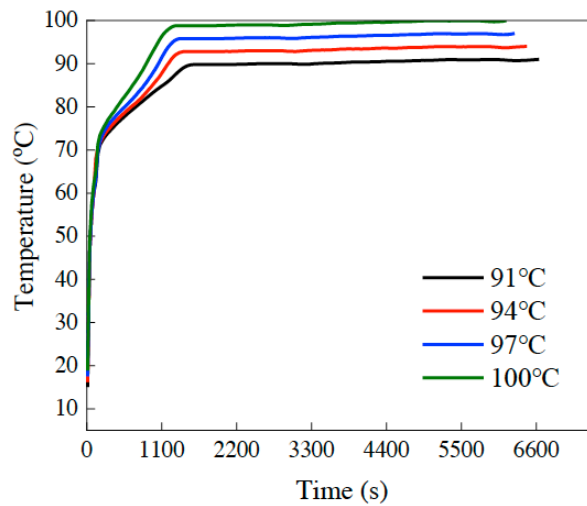
(d) 2nd Exothermic



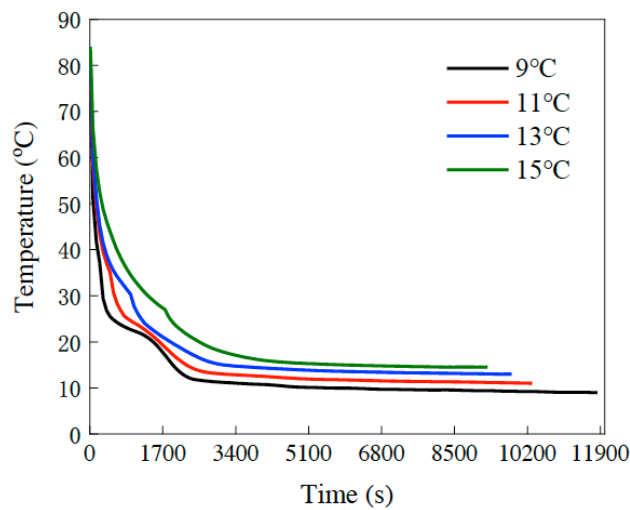
(e) 3rd Endothermic



(f) 3rd Exothermic



(g) Outlet temperature of cascaded thermal energy storage unit during endothermic process.



(h) Outlet temperature of cascaded thermal energy storage unit during exothermic process.

Figure 7: Data of cascaded thermal energy storage unit versus different heat transfer fluid temperatures: (a) 1st Endothermic, (b) 1st Exothermic, (c) 2nd Endothermic, (d) 2nd Exothermic, (e) 3rd Endothermic, (f) 3rd Exothermic, (g) Outlet temperature of cascaded thermal energy storage unit during endothermic process, (h) Outlet temperature of cascaded thermal energy storage unit during exothermic process.

$^{\circ}\text{C}$, the charging is increased by 11.17%, along with the gradually increased exergy efficiency. Exergy efficiency reached 43.24% when the HTF temperature was 100°C , while exergy efficiency increased by 2.56% compared with that of 91°C . At the same time, the higher the heat storage temperature, the higher the corresponding outlet temperature, and the higher the cascaded thermal storage unit temperature can also shorten the heat storage time. According to the above factors, when the HTF temperature is 100°C , the thermal performance of the cascaded storage system is optimized for endothermic condition.

With the decrease of the unit temperature, the LPF at the same time is also reduced, because the large temperature difference in the heat transfer process improves the heat transfer efficiency of the system, which can also be seen from the change of the outlet

temperature. The HTF temperature of 9°C is optimal when heat discharging rate is more concerned, and the corresponding was 234.69J/s. Compared with the HTF at 15°C , the discharging rate is increased by 23.69%. When focusing on system energy efficiency, the optimal exergy efficiency is 54.12% at 15°C , 1.99% higher than that of 9°C during exothermic procedure.

5. CONCLUSION

In this study, a triple staged cascaded phase change thermal energy storage unit have been manufactured, tested and optimized. And it was found that the triple cascaded phase change energy storage system has the best thermal performance, mainly in the form of large energy storage, high energy storage rate, large heat storage/release efficiency, and large exergy efficiency. The heat storage rate of cascaded phase

Table 4: Comparison Exergy Efficiency with other Studies

No.	Number of PCM Stage	Temperature Range (°C)	Exergy Efficiency (End/Exo, %)	Ref.
1	1	5-12	< 33	(Shao, Soh, Islam, & Chua, 2023)
2	2	25-85	<50	(Hassanpour, Borji, Ziapour, & Kazemi, 2020)
3	3	13-17	11-35	(Cheng & Zhai, 2018)
4	3	30-90	41.54/53.22	This study

change is significantly better than those of single stage counterpart. Besides, in the process of heat storage, the storage rate and exergy efficiency of the cascaded storage system are the highest, which are 334.95 J/s and 41.54 %, respectively. In the heat release process, the discharging rate and exergy efficiency of the system are 186.37 J/s and 53.22 %, respectively.

Moreover, the influence of HTF flowrate and temperature on the thermal performance of the system was studied in a tertiary cascaded phase change thermal energy storage system, where exergy efficiency and energy storage rate of PCMs were represented. For the endothermic process, when the flowrate is 3 L/min, the thermal performance of the system is the best. Additionally, in the process of heat release, the flow rate of 2 L /min is the best when it is applied to the situation focusing on heat release rate. While the flowrate of 1.4 L/min is optimal for applications that focus on system energy efficiency. For the HTF temperature, when the inlet temperature is 100 °C during the heat storage process, the thermal performance is the best. And in the exothermic process, the inlet temperature of 9 °C is the best when heat release rate is more concerned. However, when suitable for applications with an emphasis on system energy efficiency, an HTF temperature of 15 °C is optimal.

Comparing with other studies which have formerly conducted, the exergy of the present manuscript is quite acceptable as listed in Table 4, which also signifies that the proposed system is of competent thermal performance in relative application. Therefore, with the optimized configuration, is this storage unit a qualified candidate for thermal energy storage deployment towards building heating purpose. This case study may produce specified guide in related projects and provide practical instructional meanings.

ACKNOWLEDGEMENT

This work is supported by National Natural Science Foundation of China (No. 51978231), Natural Science Foundation of Hebei Province General Project (No. E2023202232).

REFERENCE

- Ahmed, S. D., Al-Ismael, F. S. M., Shafiullah, M., Al-Sulaiman, F. A., & El-Amin, I. M. (2020). Grid Integration Challenges of Wind Energy: A Review. *IEEE Access*, 8, 10857-10878. doi:<https://doi.org/10.1109/ACCESS.2020.2964896>
- Algarni, S., Mellouli, S., Alqahtani, T., Almutairi, K., Khan, A., & Anqi, A. (2020). Experimental investigation of an evacuated tube solar collector incorporating nano-enhanced PCM as a thermal booster. *Applied Thermal Engineering*, 180, 115831. doi:<https://doi.org/10.1016/j.applthermaleng.2020.115831>
- Bao, X., Yang, H., Xu, X., Xu, T., Cui, H., Tang, W., Fung, W. H. (2020). Development of a stable inorganic phase change material for thermal energy storage in buildings. *Solar Energy Materials and Solar Cells*, 208, 110420. doi:<https://doi.org/10.1016/j.solmat.2020.110420>
- Cao, S., Luo, X., Han, X., Lu, X., & Zou, C. (2022). Development of a New Modified CaCl₂·6H₂O Composite Phase Change Material. *Energies*, 15(3). doi:<https://doi.org/10.3390/en15030824>
- Cheng, X., & Zhai, X. (2018). Thermal performance analysis of a cascaded cold storage unit using multiple PCMs. *Energy*, 143, 448-457. doi:<https://doi.org/10.1016/j.energy.2017.11.009>
- Dheep, G. R., & Sreekumar, A. (2018). Investigation on thermal reliability and corrosion characteristics of glutaric acid as an organic phase change material for solar thermal energy storage applications. *Applied Thermal Engineering*, 129, 1189-1196. doi:<https://doi.org/10.1016/j.applthermaleng.2017.10.133>
- Hassanpour, A., Borji, M., Ziapour, B. M., & Kazemi, A. (2020). Performance analysis of a cascade PCM heat exchanger and two-phase closed thermosiphon: A case study of geothermal district heating system. *Sustainable Energy Technologies and Assessments*, 40, 100755. doi:<https://doi.org/10.1016/j.seta.2020.100755>
- Huang, M., He, W., Incecik, A., Gupta, M. K., Królczyk, G., & Li, Z. (2022). Phase change material heat storage performance in the solar thermal storage structure employing experimental evaluation. *Journal of Energy Storage*, 46, 103638. doi:<https://doi.org/10.1016/j.est.2021.103638>
- Jouhara, H., Żabnieńska-Góra, A., Khordehgah, N., Ahmad, D., & Lipinski, T. (2020). Latent thermal energy storage technologies and applications: A review. *International Journal of Thermofluids*, 5-6, 100039. doi:<https://doi.org/10.1016/j.ijft.2020.100039>
- Kumar, K., & Saini, R. P. (2022). A review on operation and maintenance of hydropower plants. *Sustainable Energy Technologies and Assessments*, 49, 101704. doi:<https://doi.org/10.1016/j.seta.2021.101704>
- Kumar, R. R., Samykano, M., Pandey, A. K., Said, Z., Kadrigama, K., & Tyagi, V. V. (2022, 21-24 Feb. 2022). Experimental Investigations on Thermal Properties of Copper (II) Oxide Nanoparticles Enhanced Inorganic Phase Change Materials for Solar Thermal Energy Storage Applications. Paper presented at the 2022 Advances in Science and Engineering Technology International Conferences (ASET).

12. Lamrani, B., Kuznik, F., & Draoui, A. (2020). Thermal performance of a coupled solar parabolic trough collector latent heat storage unit for solar water heating in large buildings. *Renewable Energy*, 162, 411-426. [doi:https://doi.org/10.1016/j.renene.2020.08.038](https://doi.org/10.1016/j.renene.2020.08.038)
13. Lancet, D., & Pecht, I. (1977). Spectroscopic and immunochemical studies with nitrobenzoxadiazolealanine, a fluorescent dinitrophenyl analog. *Biochemistry*, 16(23), 5150-5157. [doi:https://doi.org/10.1021/bi00642a031](https://doi.org/10.1021/bi00642a031)
14. Levenda, A. M., Behrsin, I., & Disano, F. (2021). Renewable energy for whom? A global systematic review of the environmental justice implications of renewable energy technologies. *Energy Research & Social Science*, 71, 101837. [doi:https://doi.org/10.1016/j.erss.2020.101837](https://doi.org/10.1016/j.erss.2020.101837)
15. Li, X., He, Y., Yin, B., Miao, Z., & Li, X. (2008). Exergy flow and energy utilization of direct methanol fuel cells based on a mathematical model. *Journal of Power Sources*, 178(1), 344-352. [doi:https://doi.org/10.1016/j.jpowsour.2007.08.019](https://doi.org/10.1016/j.jpowsour.2007.08.019)
16. Ma, Z., Bao, H., & Roskilly, A. P. (2020). Electricity-assisted thermochemical sorption system for seasonal solar energy storage. *Energy Conversion and Management*, 209, 112659. [doi:https://doi.org/10.1016/j.enconman.2020.112659](https://doi.org/10.1016/j.enconman.2020.112659)
17. Manohar, M., Koley, E., Ghosh, S., Mohanta, D. K., & Bansal, R. C. (2020). Spatio-temporal information based protection scheme for PV integrated microgrid under solar irradiance intermittency using deep convolutional neural network. *International Journal of Electrical Power & Energy Systems*, 116, 105576. [doi:https://doi.org/10.1016/j.ijepes.2019.105576](https://doi.org/10.1016/j.ijepes.2019.105576)
18. Manoj Kumar, P., Karuna, M. S., Sureshkumar, M. S., Lal Rinawa, M., Sakthivel, R., Muthukumar, K., & Kathir Malavan, E. (2023). Evaluating the effect of magnesium oxide nanoparticles on the thermal energy storage characteristics of the inorganic PCM. *Materials Today: Proceedings*. [doi:https://doi.org/10.1016/j.matpr.2023.02.297](https://doi.org/10.1016/j.matpr.2023.02.297)
19. Nekoonam, S., & Ghasempour, R. (2021). Optimization of a solar cascaded phase change slab-plate heat exchanger thermal storage system. *Journal of Energy Storage*, 34, 102005. [doi:https://doi.org/10.1016/j.est.2020.102005](https://doi.org/10.1016/j.est.2020.102005)
20. Neto, P. B. L., Saavedra, O. R., & Oliveira, D. Q. (2020). The effect of complementarity between solar, wind and tidal energy in isolated hybrid microgrids. *Renewable Energy*, 147, 339-355. [doi:https://doi.org/10.1016/j.renene.2019.08.134](https://doi.org/10.1016/j.renene.2019.08.134)
21. Nukulwar, M. R., & Tungikar, V. B. (2021). A review on performance evaluation of solar dryer and its material for drying agricultural products. *Materials Today: Proceedings*, 46, 345-349. [doi:https://doi.org/10.1016/j.matpr.2020.08.354](https://doi.org/10.1016/j.matpr.2020.08.354)
22. Pasupathi, M. K., Alagar, K., P, M. J., M.M, M., & Aritra, G. (2020). Characterization of Hybrid-nano/Paraffin Organic Phase Change Material for Thermal Energy Storage Applications in Solar Thermal Systems. *Energies*, 13(19). [doi:https://doi.org/10.3390/en13195079](https://doi.org/10.3390/en13195079)
23. Qiao, X., Kong, X., & Fan, M. (2022). Phase change material applied in solar heating for buildings: A review. *Journal of Energy Storage*, 55, 105826. [doi:https://doi.org/10.1016/j.est.2022.105826](https://doi.org/10.1016/j.est.2022.105826)
24. Qiao, X., Kong, X., Li, H., Wang, L., & Long, H. (2020). Performance and optimization of a novel active solar heating wall coupled with phase change material. *Journal of Cleaner Production*, 250, 119470. [doi:https://doi.org/10.1016/j.jclepro.2019.119470](https://doi.org/10.1016/j.jclepro.2019.119470)
25. Rabaia, M. K. H., Abdelkareem, M. A., Sayed, E. T., Elsaid, K., Chae, K.-J., Wilberforce, T., & Olabi, A. G. (2021). Environmental impacts of solar energy systems: A review. *Science of The Total Environment*, 754, 141989. [doi:https://doi.org/10.1016/j.scitotenv.2020.141989](https://doi.org/10.1016/j.scitotenv.2020.141989)
26. Ruggiero, C. A. (2021). Sustainability and sustainable development: A review of principles and definitions. *Science of The Total Environment*, 786, 147481. [doi:https://doi.org/10.1016/j.scitotenv.2021.147481](https://doi.org/10.1016/j.scitotenv.2021.147481)
27. Sami, S., Etesami, N., & Rahimi, A. (2011). Energy and exergy analysis of an indirect solar cabinet dryer based on mathematical modeling results. *Energy*, 36(5), 2847-2855. [doi:https://doi.org/10.1016/j.energy.2011.02.027](https://doi.org/10.1016/j.energy.2011.02.027)
28. Shamsi, H., Boroushaki, M., & Gerai, H. (2017). Performance evaluation and optimization of encapsulated cascade PCM thermal storage. *Journal of Energy Storage*, 11, 64-75. [doi:https://doi.org/10.1016/j.est.2017.02.003](https://doi.org/10.1016/j.est.2017.02.003)
29. Shao, Y. L., Soh, K. Y., Islam, M. R., & Chua, K. J. (2023). Thermal, exergy and economic analysis of a cascaded packed-bed tank with multiple phase change materials for district cooling system. *Energy*, 268, 126746. [doi:https://doi.org/10.1016/j.energy.2023.126746](https://doi.org/10.1016/j.energy.2023.126746)
30. Singh, P., Sharma, R. K., Ansu, A. K., Goyal, R., Sari, A., & Tyagi, V. V. (2021). A comprehensive review on development of eutectic organic phase change materials and their composites for low and medium range thermal energy storage applications. *Solar Energy Materials and Solar Cells*, 223, 110955. [doi:https://doi.org/10.1016/j.solmat.2020.110955](https://doi.org/10.1016/j.solmat.2020.110955)
31. Somu, N., Raman M R, G., & Ramaritham, K. (2021). A deep learning framework for building energy consumption forecast. *Renewable and Sustainable Energy Reviews*, 137, 110591. [doi:https://doi.org/10.1016/j.rser.2020.110591](https://doi.org/10.1016/j.rser.2020.110591)
32. Soni, V. (2021). Nanoadditive Particles segregation and mobility in phase change materials. *International Journal of Heat and Mass Transfer*, 165, 120676. [doi:https://doi.org/10.1016/j.ijheatmasstransfer.2020.120676](https://doi.org/10.1016/j.ijheatmasstransfer.2020.120676)
33. Sukarno, R., Putra, N., Hakim, I. I., Rachman, F. F., & Indra Mahlia, T. M. (2021). Utilizing heat pipe heat exchanger to reduce the energy consumption of airborne infection isolation hospital room HVAC system. *Journal of Building Engineering*, 35, 102116. [doi:https://doi.org/10.1016/j.jobbe.2020.102116](https://doi.org/10.1016/j.jobbe.2020.102116)
34. Verma, P., Varun, & Singal, S. K. (2008). Review of mathematical modeling on latent heat thermal energy storage systems using phase-change material. *Renewable and Sustainable Energy Reviews*, 12(4), 999-1031. [doi:https://doi.org/10.1016/j.rser.2006.11.002](https://doi.org/10.1016/j.rser.2006.11.002)
35. Zhang, S., Feng, D., Shi, L., Wang, L., Jin, Y., Tian, L., Yan, Y. (2021). A review of phase change heat transfer in shape-stabilized phase change materials (ss-PCMs) based on porous supports for thermal energy storage. *Renewable and Sustainable Energy Reviews*, 135, 110127. [doi:https://doi.org/10.1016/j.rser.2020.110127](https://doi.org/10.1016/j.rser.2020.110127)

Received on 01-12-2023

Accepted on 18-12-2023

Published on 30-12-2023

DOI: <https://doi.org/10.31875/2410-2199.2023.10.08>

© 2023 Qiao et al.; Zeal Press.

This is an open access article licensed under the terms of the Creative Commons Attribution License (<http://creativecommons.org/licenses/by/4.0/>) which permits unrestricted use, distribution and reproduction in any medium, provided the work is properly cited.